Ecology, 80(1), 1999, pp. 202–210

POPULATION DYNAMICS OF LIGHT-LIMITED PHYTOPLANKTON: MICROCOSM EXPERIMENTS

JEF HUISMAN

Laboratory for Microbiology, University of Amsterdam, Nieuwe Achtergracht 127, 1018 WS Amsterdam, The Netherlands; [1]
Departments of Plant Biology and Genetics, University of Groningen, P.O. Box 14, 9750 AA Haren, The Netherlands; and
Stanford University, Biological Sciences, Gilbert Hall, Stanford, CA 94305-5020, USA

Abstract. This paper investigates the extent to which the predictions of an elementary model for light-limited growth are matched by laboratory experiments with light-limited phytoplankton. The model and experiments link the population dynamics of phytoplankton species with changes in the light gradient caused by phytoplankton shading. The model predicts that a phytoplankton population should continue to grow until, at steady state, the light intensity at the bottom of the water column equals its critical light intensity. The experimental results were in good agreement with the theoretical predictions: (1) the steady-state population density increased with an increase of the incident light intensity, (2) the steady-state population density (per unit volume) was inversely proportional to mixing depth, (3) the steady-state population size (per unit area) decreased linearly with mixing depth, (4) the critical light intensity decreased with an increase of the incident light intensity, (5) the critical light intensity was approximately the same at each mixing depth, and (6) the time courses predicted by the model were in line with the observed time courses of population density and light penetration. Implications for phytoplankton ecology and aquatic production biology are discussed.

Key words: chemostat; Chlorella vulgaris; *critical light intensity; light supply; light-limited growth model; mixing depth; photosynthesis; phytoplankton; population density; population dynamics.*

INTRODUCTION

Many concepts in aquatic ecology are based on the light gradient. For example, for a given light gradient it is possible to indicate the depth of the euphotic zone, where most photosynthesis takes place (cf. Reynolds 1984). For a given light gradient it is possible to estimate the critical depth of a mixed water column that just allows phytoplankton growth (Sverdrup 1953). For a given light gradient, mathematical expressions are available to calculate depth-integrated primary production (Talling 1957, Fee 1969, Platt et al. 1990, Anderson 1993). There is a problem, however. When phytoplankton populations increase, they will absorb more light, and the light gradient will change (Talling 1960, Jewson 1977, Dubinsky and Berman 1981, Tilzer et al. 1994). In this way, a change in the phytoplankton causes a change in the depth of the euphotic zone, a change in the critical depth, and a change in depth-integrated primary production. A dynamic description of the light gradient will be required to predict the density-dependent development of phytoplankton blooms or the successive replacement of phytoplankton species during competition.

Manuscript received 27 August 1997; revised 20 February 1998; accepted 11 March 1998.
[1] Address for correspondence.
E-mail: jef.huisman@chem.uva.nl

We developed a model for light-limited growth and competition for light in well mixed aquatic environments (Huisman and Weissing 1994, 1995, Weissing and Huisman 1994). The model is based on standard assumptions. The light gradient is described by Lambert–Beer's law, and depth integrals are used to calculate depth-integrated production. In this sense, the model is only a simple extension of many earlier production models (e.g., Sverdrup 1953, Talling 1957, Platt et al. 1990, Kirk 1994). The emphasis is different, however. It is a dynamic model that emphasizes the coupling between changes in phytoplankton population density and changes in the light gradient caused by phytoplankton shading. The model predicts that if light conditions are favorable for growth, the phytoplankton population will increase. An increased phytoplankton population will absorb more light, and thus create a steeper light gradient. Accordingly, the overall light conditions become less favorable for growth, and the net phytoplankton growth rate diminishes. This continues until light conditions are such that the phytoplankton population no longer increases. A steady state has been reached, with a characteristic population density and a characteristic light gradient.

The steady-state light intensity at the bottom of the water column has been termed the critical light intensity (Huisman and Weissing 1994). The critical light intensity is species specific and plays a crucial role

when phytoplankton species compete for light. Theory predicts that the species with lowest critical light intensity should be the superior light competitor (Huisman and Weissing 1994, Weissing and Huisman 1994). Recent competition experiments confirm this prediction (Huisman et al. 1999).

The steady-state population density and the critical light intensity depend on environmental factors like light supply, mixing depth, and background turbidity. More precisely, the model predicts the following environmental patterns: (1) the steady-state population density should increase with increasing light supply, (2) the steady-state population density (per unit volume) should be inversely proportional to mixing depth, (3) the steady-state population size (per unit area) should decrease linearly with mixing depth, (4) the critical light intensity should decrease with increasing light supply, (5) the critical light intensity should be independent of mixing depth. Here I report on tests of these predictions using microcosm experiments with the green alga *Chlorella vulgaris.*

Theory

Consider a well-mixed water column. Let ω denote the phytoplankton population density, with dimension being number of phytoplankton per unit volume. The growth rate of the phytoplankton population depends on the balance between production and losses:

$$\frac{d\omega}{dt} = \frac{1}{z}\int_0^z p[I(s)]\omega\, ds - D\omega \tag{1}$$

where $p(I)$ is the specific rate of production as an increasing function of light intensity, $I(s)$ is the light intensity as a decreasing function of depth s, z is the total depth of the water column, and D is the loss rate imposed by dilution.

The light intensity, I, decreases with depth s according to Lambert-Beer's law:

$$I(s) = I_{\text{in}}e^{-(k\omega s + K_{\text{bg}}s)} \tag{2}$$

where I_{in} is the incident light intensity, k is the specific light attenuation coefficient of the phytoplankton, and K_{bg} is the total background turbidity due to nonphytoplankton components. The light intensity at the bottom of the water column, I_{out}, is given by $I_{\text{out}} = I(z)$.

Combining Eqs.1 and 2 gives the following dynamical system (Huisman and Weissing 1994, Weissing and Huisman 1994; see also Bannister 1974):

$$\frac{d\omega}{dt} = \frac{1}{z}\frac{k\omega}{(k\omega + K_{\text{bg}})}\int_{I_{\text{out}}}^{I_{\text{in}}}\frac{p(I)}{kI}\,dI - D\omega \tag{3a}$$

$$I_{\text{out}} = I_{\text{in}}e^{-(k\omega z + K_{\text{bg}}z)}. \tag{3b}$$

This model predicts that there is a critical value of I_{out}, which we have called the critical light intensity, at which the phytoplankton population should remain stationary (Huisman and Weissing 1994, Weissing and Huisman 1994). The phytoplankton population should increase as long as I_{out} is above its critical light intensity, whereas the population should decrease as soon as I_{out} is below its critical light intensity. These population dynamics lead to a steady state. A phytoplankton population should grow until, at steady state, it has reduced the light intensity at the bottom of the water column to its critical light intensity.

Light supply

It comes as no surprise that Eqs. 3a and b predict that the steady-state population density should be an increasing function of the light supply. More surprisingly, an increase of the light supply should also lead to a lower critical light intensity. The intuition is as follows (formal proofs are given in Huisman and Weissing 1994, Weissing and Huisman 1994). A steady state is reached when the net photosynthetic gains in the upper part of the water column are exactly balanced by net losses at the lower part. When the light supply is increased, this yields more gains in the top of the water column. Hence, the phytoplankton population will grow further, until these additional gains in the top of the water column are balanced by additional losses at the bottom. Additional losses at the bottom will occur when the light intensity at the bottom is reduced to lower levels. That is, the critical light intensity, which is measured at the bottom, should become lower.

Mixing depth

A limited light supply per unit area can sustain only a limited number of phytoplankton cells per unit area. When the mixing depth of a water column is increased, this limited amount of phytoplankton is diluted over a deeper column of water. Thus, one should expect that under light-limited conditions the population density would be negatively correlated with mixing depth. This intuitive reasoning conforms to the model's predictions. Eqs. 3a and b predict that the critical light intensity is independent of mixing depth (Huisman and Weissing 1994, Weissing and Huisman 1994). Because the critical light intensity is independent of mixing depth, it follows from Eq. 3b that the population density (in cells/cm^3) at steady state should be inversely proportional to mixing depth:

$$\omega^* = \frac{1}{kz}\ln(I_{\text{in}}/I^*_{\text{out}}) - \frac{K_{\text{bg}}}{k} \tag{4}$$

where I^*_{out} is the critical light intensity, and ω^* indicates that ω is evaluated at steady state.

Also the number of phytoplankton cells per unit area, W, is related to mixing depth. All else being equal, in a deeper water column, more light is absorbed by water and other nonphytoplankton components. Hence less light remains for phytoplankton. More precisely, from Eq. 4 it follows that the population size per unit area (cells/cm^2) at steady state should decrease linearly with mixing depth:

$$W^* = \omega^* z = \frac{1}{k}\ln(I_{in}/I^*_{out}) - \frac{K_{bg}}{k}z. \quad (5)$$

Note that the decrease of population size with increasing mixing depth is caused by the background turbidity due to nonphytoplankton components. The population size per unit area would remain constant when background turbidity, K_{bg}, were zero.

Generality

Weissing and Huisman (1994) showed that this theory holds for all $p(I)$ functions proposed in the literature (as reviewed by Jassby and Platt 1976, Henley 1993), except for those considering photoinhibition. Photoinhibition introduces some new dynamical phenomena that will be addressed in further study.

Methods

Culture methods

The experiments were performed with unialgal (but nonaxenic) cultures of the unicellular green alga *Chlorella vulgaris* Beyerinck. This species was grown in continuous-culture systems developed for the study of light-limited phytoplankton. The culture system is described in detail in Huisman et al. (1999), and only a short résumé is given here. Each continuous culture consisted of a flat culture vessel, illuminated from one side to create a unidirectional light gradient. To investigate various mixing depths, culture vessels had optical path lengths, ''mixing depths,'' of $z = 3.2$ cm, 5 cm, 10 cm, and 20 cm. The effective working volumes of these vessels were 1100 mL, 1600 mL, 3225 mL, and 6550 mL, respectively. A water jacket placed between the light source and the culture vessel maintained the temperature of the culture vessel at 20°C. Homogeneous mixing of the cultures and a sufficient supply of CO_2 were ensured by bubbling air between two partitions within the culture vessel at a rate of 100–150 L/h. The 20 cm-deep vessel had two air inlets, and the other vessels had only one. Cultures were supplied with excess nutrients (Huisman et al. 1999). Pilot experiments showed that neither halving nor doubling of the nutrient dosage had an effect on steady-state population densities, indicating that nutrients were neither limiting nor present in toxic amounts. The continuous cultures were run at a dilution rate of $D = 0.02$ h^{-1}. Light intensities (PAR, in μmol photons·m^{-2}·s^{-1}) were measured with a Licor LI-190SA quantum sensor. The light intensity incident upon the culture vessel (I_{in}) was set by neutral density filters. The light intensity I_{out} was measured as the light intensity leaving the culture vessel at the back surface. To account for spatial variation, I_{out} was sampled at 10 regularly spaced positions at the back surface. Critical light intensities were measured as the values of I_{out} observed when the cultures were in steady state. Cultures were sampled nearly every day, and population densities were counted in triplo with a Coulter Counter (model ZM) directly after sampling.

Quantitative analysis

The qualitative theory holds for nearly all $p(I)$ functions proposed in the literature (Weissing and Huisman 1994). To test quantitative aspects of the theory, it is necessary to choose a particular $p(I)$ function to quantify the dependence of specific production on light intensity. Numerous $p(I)$ functions have been proposed (e.g., Jassby and Platt 1976, Henley 1993). At present, the $p(I)$ function proposed by Webb et al. (1974) and Platt et al. (1980) is probably most often used. However, this $p(I)$ function has no closed-form solution of its depth integral, and this causes problems in parameter estimation. I estimated parameters by fitting differential equations (Eqs. 7a and b) to the time courses of the experiments. This advanced technique consumes a lot of computation time, even on a fast computer, because it is an iterative procedure (Richter and Söndgerath 1990). At each iteration, the differential equations have to be solved numerically. Consider the use of the $p(I)$ function of Platt et al. (1980). Numerical expressions are available to approximate its depth integral (Platt et al. 1991). However, an additional numerical procedure might introduce additional error in the fitting procedure, and the computation time would increase enormously. Therefore, I have chosen for the Monod equation

$$p(I) = \frac{p_{max} I}{(p_{max}/\alpha) + I} \quad (6)$$

where p_{max} is the maximum rate of specific production, and α is the slope of the $p(I)$ function at $I = 0$. The advantage of the Monod equation is that it has a simple analytical solution of its depth integral. In fact, substituting Eq. 6 in Eq. 3a, the dynamics of phytoplankton growth reads (Huisman and Weissing 1994):

$$\frac{d\omega}{dt} = \frac{1}{z}\frac{k\omega}{(k\omega + K_{bg})}\frac{p_{max}}{k}\ln\left(\frac{p_{max} + \alpha I_{in}}{p_{max} + \alpha I_{out}}\right) - D\omega \quad (7a)$$

$$I_{out} = I_{in} e^{-(k\omega z + K_{bg} z)}. \quad (7b)$$

This quantitative model was fit to the data. The parameters I_{in}, z, and D were measured directly. The background turbidity was calculated from measurements of I_{in} and I_{out} in the absence of phytoplankton according to $K_{bg} = \ln(I_{in}/I_{out})/z$. The remaining parameters, p_{max}, α, and k, were estimated by a least-squares fit of model predictions vs. observed values of population density and I_{out}, as outlined above. The least-squares fit was performed only once, over the complete data set (a total of 192 paired observations of population density and I_{out}).

Results

Light supply

Continuous cultures, with culture vessels 5 cm deep, were run at seven different incident light intensities.

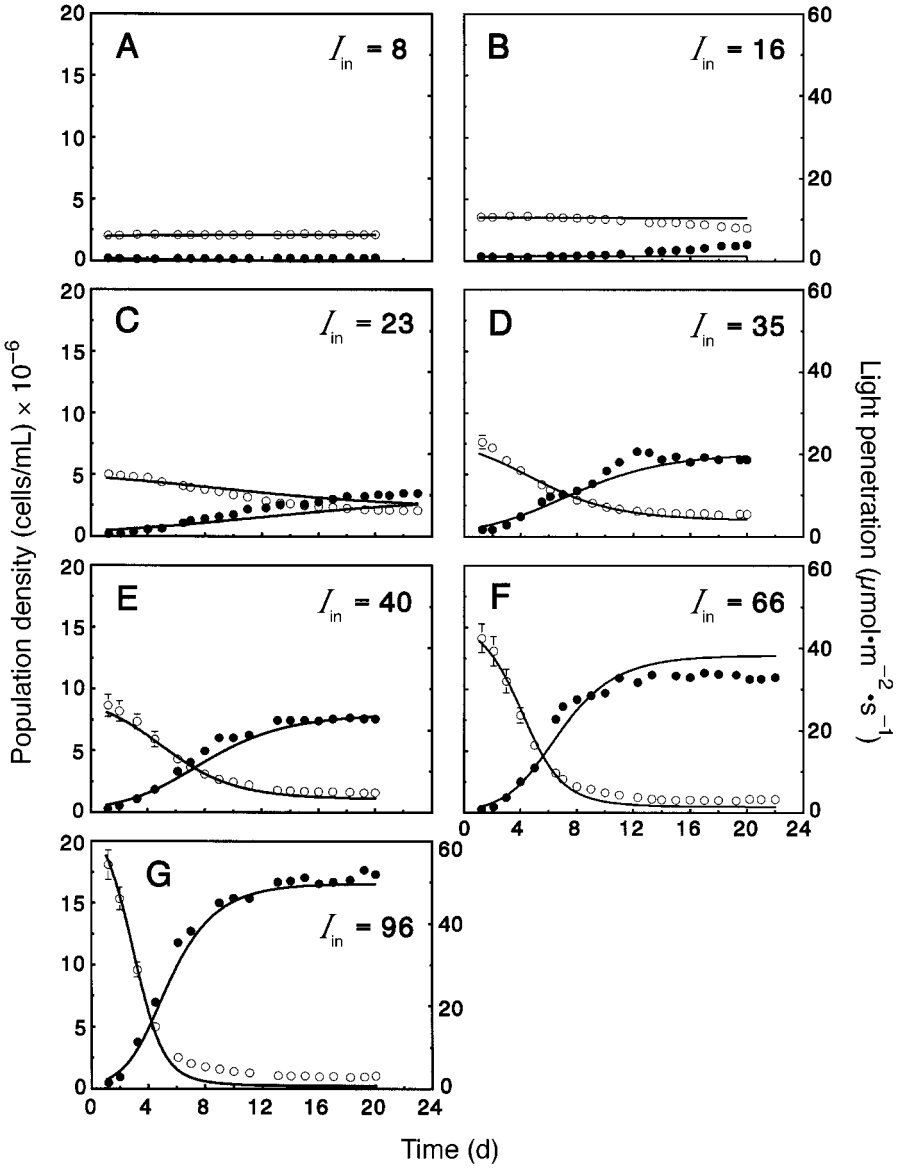

FIG. 1. Time course of population density (●) and light intensity I_{out} (○) at different incident light intensities. Error bars indicate the spatial standard deviation of I_{out} ($N = 10$). When not visible, the spatial standard deviation did not exceed the size of the circle. Solid lines show the time course predicted by Eqs. 7a and b. The incident light intensity (I_{in}, in μmol·m^{-2}·s^{-1}) is indicated in each subfigure. Remaining system parameters: $z = 5.0$ cm; $K_{bg} = 0.068$ cm^{-1}; $D = 0.020$ h^{-1}. Species parameters: $p_{max} = 0.0756$ h^{-1}; $\alpha = 0.00212$ h^{-1} (μmol·m^{-2}·s^{-1})$^{-1}$; $k = 5.47 \times 10^{-8}$ cm^2/cell.

Fig. 1 shows the time course of population density and I_{out} during these experiments. At an incident light intensity of 8 μmol·m^{-2}·s^{-1}, the light input was too low to sustain a phytoplankton population (Fig. 1A). In all other experiments, the light input was high enough to enable phytoplankton growth (Fig. 1B–G). In each experiment, population density increased and I_{out} decreased until a steady state was reached after 12–18 d. The solid lines show that Eqs. 7a and b fit quite well to the data. At the higher incident light intensities the predicted values of I_{out} are slightly lower than the observed values.

Critical light intensity and steady-state population density were calculated as the average I_{out} and average population density, respectively, over the last five days of each experiment. Qualitatively, the steady-state population density increased significantly with the light supply (Fig. 2A; Spearman rank correlation: $r_S = 1$, $N = 7$, $P < 0.002$). This demonstrates that the population density was indeed limited by light. Quantitatively, the model predictions of steady-state population density (solid line in Fig. 2A) agree well with the observed steady-state population densities.

As should be expected from Lambert–Beer's law,

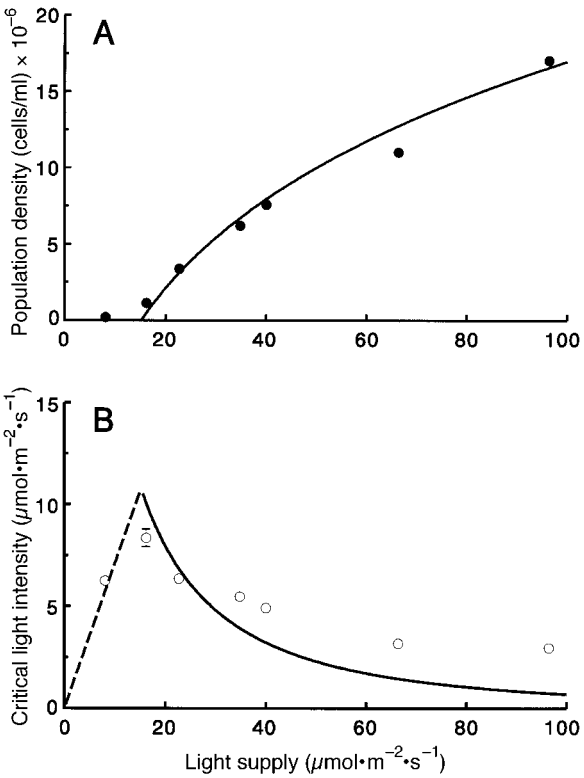

FIG. 2. (A) Steady-state population density, and (B) critical light intensity in relation to the light supply. These values were calculated as the average population density and average I_{out} over the last 5 d of each experiment in Fig. 1. Error bars indicate SD ($N = 5$). When not visible, the SD did not exceed the size of the circle. Solid lines are based on equilibrium solutions of Eqs. 7a and b, using the parameter values of Fig. 1. The dashed line in (B) gives the relation between I_{in} and I_{out} in the absence of phytoplankton.

without phytoplankton I_{out} increased linearly with I_{in} (linear regression forced through the origin: $I_{out} = 0.71I_{in}$, $N = 15$, $r^2 = 0.99$, $P < 0.001$). This linear relation is indicated by the dashed line in Fig. 2B. The experiment at $I_{in} = 8$ μmol·m^{-2}·s^{-1} falls on this line. In all other experiments, the light supply was sufficiently high to enable phytoplankton growth. For these experiments, the critical light intensity decreased significantly with an increase of the light supply (Fig. 2B; Spearman rank correlation: $r_S = 1$, $N = 6$, $P < 0.01$). Thus, qualitatively, these observations are in line with the theoretical prediction that the critical light intensity should decrease with an increase of the light supply. Quantitatively, however, there is a rather poor fit between the observed and predicted critical light intensities. Especially at a high light supply, the model predicts a lower critical light intensity than actually observed (Fig. 2B).

I also tested for the critical light intensities of a few other species. Two green algae (*Chlorella vulgaris* and *Scenedesmus protuberans*), two cyanobacteria (*Aphanizomenon flos-aquae* and a *Microcystis* strain), and a diatom (*Cylindrotheca closterium*) were cultured, using the same experimental setup, at both a low and a high light supply. The dilution rate in these experiments was set at $D = 0.015$ h^{-1} to ensure that all species could thrive. For all five species the critical light intensity was lower at a high light supply than at a low light supply (Table 1). The probability, P, that this would happen by chance for all five species is $P = (1/2)^5 \approx 0.03$. Hence, the pattern was significant at the 0.05 level.

TABLE 1. Critical light intensities (means, with 1 SD in parentheses) of (A) two green algae (*Chlorella vulgaris* and *Scenedesmus protuberans*), two cyanobacteria (*Aphanizomenon flos-aquae* and *Microcystis* sp.), and (B) a diatom (*Cylindrotheca closterium*) at two different incident light intensities.

A)	Critical light intensity	
Species	$I_{in} = 30$ μmol·m^{-2}·s^{-1}	$I_{in} = 60$ μmol·m^{-2}·s^{-1}
Chlorella	3.05 (0.06)	2.75 (0.11)
Scenedesmus	9.77 (0.50)	6.49 (0.17)
Aphanizomenon	3.56 (0.16)	2.44 (0.09)
Microcystis	4.63 (0.13)	2.77 (0.08)
B)	Critical light intensity	
Species	$I_{in} = 37$ μmol·m^{-2}·s^{-1}	$I_{in} = 53$ μmol·m^{-2}·s^{-1}
Cylindrotheca†	1.86 (0.12)	1.31 (0.06)

Notes: All species were grown at a dilution rate of $D = 0.015$ h^{-1}. Critical light intensities were measured in monocultures at steady state and calculated as the average I_{out} over 7 days. $N = 7$.

† This marine diatom was cultured in saline medium (f/2-medium; Guillard and Ryther 1962).

Mixing depth

To investigate effects of mixing depth, I used four continuous cultures with culture vessels of 3.2-cm, 5-cm, 10-cm, and 20-cm deep, respectively. In all four experiments the incident light intensity was 34.5 μmol·m^{-2}·s^{-1}. Fig. 3 shows the time course of population density and I_{out} for these experiments. At the onset of the experiments, I_{out} was lowest in the deepest vessel (as should be expected from Lambert–Beer). Within 12 to 15 d, I_{out} converged to approximately the same value in all four vessels, and a steady state was reached. Population densities became very high in the vessel of 3.2 cm-deep, were intermediate in the vessels of 5-cm and 10-cm deep, and remained rather low in the vessel of 20-cm deep. Eqs. 7a and b fit fairly well to the data (Fig. 3).

Critical light intensity, steady-state population density (number of phytoplankton/cm^3), and steady-state population size (number of phytoplankton per cm^2) were calculated as the average I_{out}, average population density and average population size, respectively, over the last five days of each experiment. The critical light intensity did not show a clear pattern in relation to mixing depth (Fig. 4A). It ranged from 6.9 μmol·m^{-2}·s^{-1}

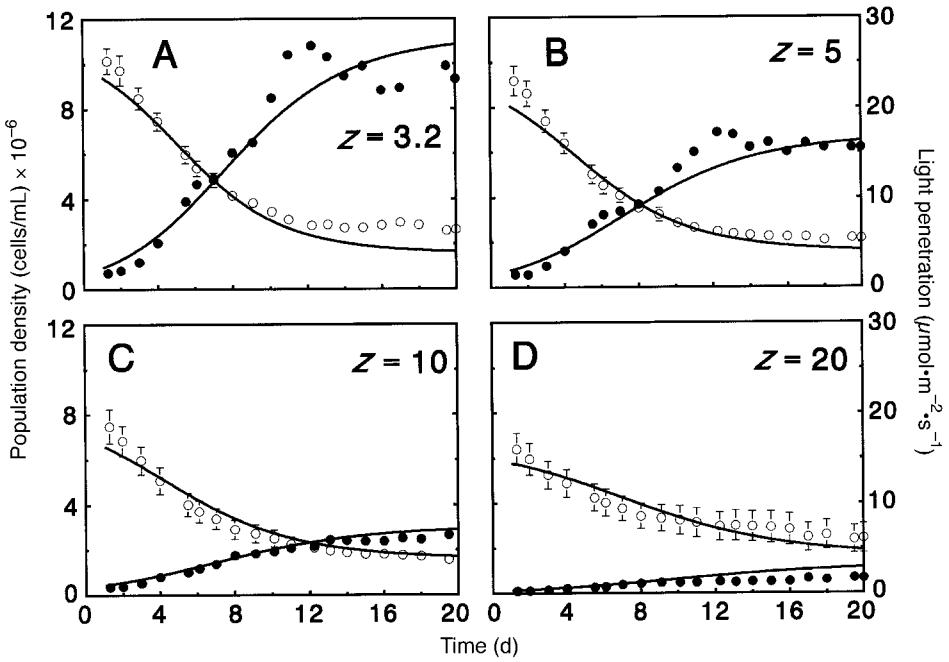

FIG. 3. Time course of population density (●) and light intensity I_{out} (○) at different mixing depths. Error bars indicate the spatial SD of I_{out} ($N = 10$). When not visible, the spatial SD did not exceed the size of the circle. Solid lines show the time course predicted by Eqs. 7a and b. The mixing depth (z, in cm) is indicated in each subfigure. Remaining system parameters: (A) $K_{bg} = 0.070$ cm^{-1}, (B) $K_{bg} = 0.072$ cm^{-1}, (C) $K_{bg} = 0.050$ cm^{-1}, (D) $K_{bg} = 0.035$ cm^{-1}; (A–D) $I_{in} = 34.5$ μmol·m^{-2}·s^{-1}; $D = 0.020$ h^{-1}. Species parameters are as in Fig. 1.

in the 3-cm vessel to 4.3 μmol·m^{-2}·s^{-1} in the 10-cm-deep vessel. Averaged over all four experiments, the critical light intensity equaled 5.8 μmol·m^{-2}·s^{-1} (dashed line in Fig. 4A). The quantitative model predicted a somewhat lower critical light intensity (4.0 μmol·m^{-2}·s^{-1}; solid line in Fig. 4A).

The steady-state population density was inversely proportional to mixing depth (Fig. 4B), whereas the steady-state population size per unit area decreased linearly with mixing depth (Fig. 4C). Quantitatively, Eqs. 7a and b predicted slightly higher values of steady-state population density and population size than were actually observed (solid lines in Fig. 4B, C). Better accordance with the steady-state data was obtained by a direct fit of Eqs. 4 and 5 (dashed lines in Fig. 4B, C; based on linear regression of population size vs. mixing depth: $r^2 = 0.97$, $N = 4$).

DISCUSSION

An advantage of laboratory microcosms is that they allow the study of processes of interest in isolation from many other processes that play a role in the field. Hence, microcosms are ideal systems to test the internal consistencies of ecological models and theories (Gause 1934, Daehler and Strong 1996, Bohannan and Lenski 1997). The experimental results reported here were in good agreement with the theoretical hypotheses. As predicted, population densities increased with the light supply (Fig. 2A) and were inversely proportional to mixing depth (Fig. 4B). Population size per unit area decreased linearly with mixing depth (Fig. 4C). Critical light intensities decreased with light supply (Fig. 2B, Table 1), and remained approximately constant with mixing depth (Fig. 4A). Also, the model quantitatively fit the population densities and kept track of changes in light penetration caused by phytoplankton shading (Figs. 1, 3). Note that the model was fit to all experiments at once. Only three parameter estimates were used to describe the complete data set. This shows that the model is quantitatively consistent with the data over a relatively wide range of incident light intensities and mixing depths.

A few experimental results deviated from the theory, however. First, the experiments showed that the critical light intensity was approximately but not exactly the same at the four different mixing depths (Fig. 4A). The residual variation might be due to a physiological response to the mixing regimes. Algal cells traveling at the same velocity experience a faster oscillating light regime in a shallowly mixed layer than in a deeply mixed layer. It is conceivable that the cells adapt to these fluctuations in light intensity (Cullen and Lewis 1988, Ibelings et al. 1994), and thus they respond differently in water columns of different mixing depths. If this form of photoadaptation played a role in the experiments, however, it is not clear why this did not yield a monotonic relation between critical light intensity and mixing depth. The residual variation might also

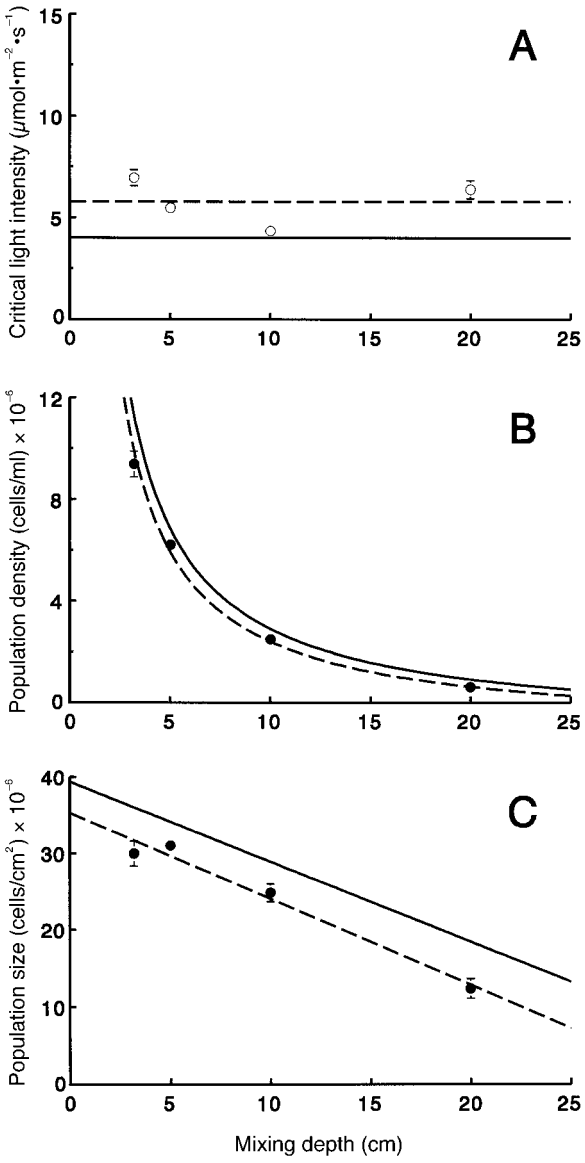

FIG. 4. (A) Critical light intensity, (B) steady-state population density, and (C) steady-state population size per unit area in relation to mixing depth. These values were calculated from the average I_{out} and average population density over the last 5 d of each experiment in Fig. 3. Error bars indicate ±1 SD ($N = 5$). When not visible, the error bar did not exceed the size of the circle. Solid lines are based on equilibrium solutions of Eqs. 7a and b, with $I_{in} = 34.5$ μmol·m^{-2}·s^{-1}, $K_{bg} = 0.057$ cm^{-1}, $D = 0.020$ h^{-1}, and the species parameters given in Fig. 1. The dashed line in (A) is the average critical light intensity observed in the four experiments (5.8 μmol·m^{-2}·s^{-1}). The dashed lines in (B) and (C) are direct fits of Eqs. 4 and 5, respectively. Using $I_{in} = 34.5$ μmol·m^{-2}·s^{-1} and $I^*_{out} = 5.8$ μmol·m^{-2}·s^{-1}, these direct fits gave the following parameter estimates: $K_{bg} = 0.057$ cm^{-1}; $k = 5.06 \times 10^{-8}$ cm^2/cell.

be an experimental artifact related to the geometry of the vessels. Bubbling with air slightly distorted the light gradient. The fraction of the culture volume that was filled with air bubbles decreased with increasing depth of the culture vessel. The deepest vessel of 20 cm, however, had two air inlets whereas the other vessels had only one. Hence, the bubbling regime might also be responsible for the variation in Fig. 4A.

Second, at a high incident light intensity the model predicted lower critical light intensities than actually observed (Fig. 2B). This pattern is probably related to the absorption spectra of the phytoplankton. Green algae hardly absorb green light. This was clearly visible in the experiments: light penetrating through the cultures was of a bright green color. Light intensities were measured, however, over the entire photosynthetically active waveband (400–700 nm). Hence, the measured critical light intensity included green light that was not well available for the algae. As a consequence, the measurements may have given a slightly higher critical light intensity than the model predicts.

A disadvantage of microcosm experiments is that they are performed at very small scales when compared to the field situation (Carpenter 1996). For example, in my experiments mixing depths did not exceed 20 cm, mixing times were on the order of a few seconds, population densities were high, the nutrient dosage was high, and incident light intensities were low. Scaling rules that facilitate translation from microcosms to the field are still in their infancy. The experiments themselves, however, suggest some fundamental scaling relationships for maximum phytoplankton carrying capacities in relation to light supply and mixing depth (Figs. 2A, 4B, C). These scaling arguments are confirmed by recent results of Petersen et al. (1997). They found that primary production per unit volume was inversely proportional to mixing depth in light-limited mesocosms with mixing depths of 45–215 cm and mixing times of 4–39 min. Primary production per unit volume was strongly correlated with chlorophyll *a* concentration in these mesocosms (J. Petersen, *personal communication*). This indicates that the scaling patterns for primary production and population density in their experiments were the same as the scaling pattern in Fig. 4B.

Several investigators have used the concept of a euphotic depth to calculate phytoplankton carrying capacities under light-limited conditions (e.g., Talling 1965, Jewson 1977, Reynolds 1984). The euphotic depth is usually defined as the depth at which the light intensity falls to 1% of the incident light. This 1% criterion implies $\ln(I_{in}) - \ln(I_{out}) = 4.6$. A correction is often made for the spectral variation in light attenuation, reducing the value from 4.6 to 3.7 (Talling 1965, Reynolds 1984). Hence, upon rearranging Lambert–Beer's law and neglecting background turbidity, the following maximum sustainable population density is obtained:

$$\omega^* = \frac{3.7}{kz}. \quad (8)$$

This equation states that the population density should be inversely proportional to mixing depth, as in Eq. 4. There are, however, two fundamental differences. First, the predictions are different. Adopting my parameter estimates for k and z, Eq. 8 predicts much higher population densities than are observed in the experiments (Fig. 4B). Also, Eq. 8 predicts that maximum sustainable population densities should be independent of the light supply. This is in conflict with common sense, and contrasts with the theory and data presented here (Fig. 2A). Second, the derivations are different. Eq. 8 is based on the assumption that I_{out} is a fixed percentage of the incident light intensity. In contrast, the critical light intensity in Eq. 4 is derived from the underlying phytoplankton dynamics. This shows that the critical light intensity is not a fixed percentage of I_{in}, but a complex function of phytoplankton characteristics and environmental parameters. Thus, it seems that Eq. 4 provides a much-improved estimator for phytoplankton carrying capacities.

Interestingly, the ratio of euphotic depth (z_{eu}) to mixing depth (z_m) can be used to make quantitative predictions. This works because the ratio z_{eu}/z_m provides sufficient information to reconstruct the light gradient. Note that z_{eu}/z_m changes with a change in population density. With some algebra, it can be derived from Lambert–Beer's law and the concept of a critical light intensity, I^*_{out}, that there is a critical ratio z_{eu}/z_m at which the population density should remain stationary:

$$\left.\frac{z_{eu}}{z_m}\right|^* = \frac{4.6}{\ln(I_{in}) - \ln(I^*_{out})} \quad (9)$$

where the value 4.6 stems from the 1% definition of the euphotic depth. Eq. 9 states that the concept of a critical light intensity is fully compatible with the concept of a critical z_{eu}/z_m ratio. One measure can be calculated from the other, and vice versa. It follows that the critical z_{eu}/z_m ratio is species specific, and that it decreases with light supply but is independent of mixing depth and background turbidity. Interestingly, several researchers have used field data on z_{eu}/z_m ratios to estimate the light requirements of phytoplankton species. Wofsy (1983), for example, presented data from a variety of eutrophic rivers, estuaries, and coastal upwelling zones. He showed that, owing to phytoplankton growth, the light conditions in these nutrient-saturated systems approach a steady state at which z_{eu}/z_m remains more or less the same independent of background turbidity and mixing depth (as in Fig. 4A). Mur and Schreurs (1995) observed that in three different eutrophic lakes, *Oscillatoria* species became dominant at the same z_{eu}/z_m ratio of approximately 0.7. Other studies that used the z_{eu}/z_m ratio to characterize the light requirements of phytoplankton species include Reynolds (1984), Kilham et al. (1986), and Sommer (1993). This suggests that the theory tested here is at least qualitatively consistent with the behavior of several natural systems, and indicates that the z_{eu}/z_m ratio may provide a useful vehicle to extrapolate from the lab to the field.

Sverdrup (1953) introduced the concept of a critical depth to estimate the onset of a phytoplankton bloom. The critical depth concept has attracted much recent debate in oceanography (Smetacek and Passow 1990, Nelson and Smith 1991, Platt et al. 1991). The debate does not mention, however, that this concept is prone to confusion because there are two possible definitions of critical depth. The critical depth is usually defined as the maximal depth of a mixed surface layer that still allows *phytoplankton growth* ($dW/dt > 0$). A problem with this definition is the feedback between phytoplankton growth and light availability. A growing phytoplankton population reduces the critical depth by shading itself. Alternatively, one might define the critical depth as the maximal mixing depth that is still able to support a *phytoplankton population* ($W^* > 0$). Thus defined the critical depth is independent of the transient dynamics of the phytoplankton but is still dependent on environmental factors like light supply and background turbidity. In fact, using the latter definition and Eq. 5, the critical depth, z_{cr}, can be calculated from the critical light intensity as

$$z_{cr} = \frac{\ln(I_{in}) - \ln(I^*_{out})}{K_{bg}}. \quad (10)$$

This equation states that the critical depth corresponds to the depth at which the critical light intensity would be reached in the absence of phytoplankton. When a water column is mixed to greater depth, the background turbidity alone imposes light conditions too dark to support a phytoplankton population. For example, extrapolation of the trend in Fig. 4C points at a critical depth of about 31 cm for the experimental conditions reported here. Interestingly, the two different definitions arrive at exactly the same prediction if application is restricted to the onset of a phytoplankton bloom (since $dW/dt > 0$ when $W \approx 0$ implies $W^* > 0$, and vice versa), in accordance with Sverdrup's (1953) original intentions. The two definitions arrive at different predictions, however, when phytoplankton is present. In the past, these two different interpretations of the concept of critical depth have not been well recognized and distinguished.

Acknowledgments

I thank Hans Balke and Hans Matthijs for practical advice and Cor Zonneveld for his contribution to the quantitative analysis. The *Cylindrotheca* data in Table 1 were provided by Stef van Bergeijk. The manuscript benefited from comments by Jelte van Andel, Carol Folt, Hans Matthijs, Luuc Mur, Joan Roughgarden, Franjo Weissing, and the anonymous reviewers. The investigations were supported by the Life Sciences Foundation (SLW), which is subsidized by the Netherlands Organization for Scientific Research (NWO), and by a TALENT-grant from NWO.

Literature Cited

Anderson, T. R. 1993. A spectrally averaged model of light penetration and photosynthesis. Limnology and Oceanography **38**:1403–1419.

Bannister, T. T. 1974. Production equations in terms of chlorophyll concentration, quantum yield, and upper limit to production. Limnology and Oceanography **19**:1–12.

Bohannan, B. J. M., and R. E. Lenski. 1997. Effect of resource enrichment on a chemostat community of bacteria and bacteriophage. Ecology **78**:2303–2315.

Carpenter, S. R. 1996. Microcosm experiments have limited relevance for community and ecosystem ecology. Ecology **77**:677–680.

Cullen, J. J., and M. R. Lewis. 1988. The kinetics of algal photoadaptation in the context of vertical mixing. Journal of Plankton Research **10**:1039–1063.

Daehler, C. C., and D. R. Strong. 1996. Can you bottle nature? The roles of microcosms in ecological research. Ecology **77**:663–664.

Dubinsky, Z., and T. Berman. 1981. Light utilization by phytoplankton in Lake Kinneret (Israel). Limnology and Oceanography **26**:660–670.

Fee, E. J. 1969. A numerical model for the estimation of photosynthetic production, integrated over time and depth, in natural waters. Limnology and Oceanography **14**:906–911.

Gause, G. F. 1934. The struggle for existence. Williams and Wilkins, Baltimore, Maryland, USA.

Guillard, R. R. L., and J. H. Ryther. 1962. Studies on marine planktonic diatoms. I. *Cyclotella nana* Hustedt and *Detonula confervacea* (Cleve) Gran. Canadian Journal of Microbiology **8**:229–239.

Henley, W. J. 1993. Measurement and interpretation of photosynthetic light-response curves in algae in the context of photoinhibition and diel changes. Journal of Phycology **29**: 729–739.

Huisman, J., R. R. Jonker, C. Zonneveld, and F. J. Weissing. 1999. Competition for light between phytoplankton species: experimental tests of mechanistic theory. Ecology **80**: 211–222.

Huisman, J., and F. J. Weissing. 1994. Light-limited growth and competition for light in well-mixed aquatic environments: an elementary model. Ecology **75**:507–520.

Huisman, J., and F. J. Weissing. 1995. Competition for nutrients and light in a mixed water column: a theoretical analysis. American Naturalist **146**:536–564.

Ibelings, B. W., B. M. A. Kroon, and L. R. Mur. 1994. Acclimation of photosystem II in a cyanobacterium and a eukaryotic green alga to high and fluctuating photosynthetic photon flux densities, simulating light regimes induced by mixing in lakes. New Phytologist **128**:407–424.

Jassby, A. D., and T. Platt. 1976. Mathematical formulation of the relationship between photosynthesis and light for phytoplankton. Limnology and Oceanography **21**:540–547.

Jewson, D. H. 1977. Light penetration in relation to phytoplankton content of the euphotic zone of Lough Neagh, North Ireland. Oikos **28**:74–83.

Kilham, P., S. S. Kilham, and R. E. Hecky. 1986. Hypothesized resource relationships among African planktonic diatoms. Limnology and Oceanography **31**:1169–1181.

Kirk, J. T. O. 1994. Light and photosynthesis in aquatic ecosystems. Second edition. Cambridge University Press, Cambridge, UK.

Mur, L. R., and H. Schreurs. 1995. Light as a selective factor in the distribution of phytoplankton species. Water Science and Technology **32**:25–34.

Nelson, D. M., and W. O. Smith, Jr. 1991. Sverdrup revisited: critical depths, maximum chlorophyll levels, and the control of Southern Ocean productivity by the irradiance-mixing regime. Limnology and Oceanography **36**:1650–1661.

Petersen, J. E., C. C. Chen, and W. M. Kemp. 1997. Scaling aquatic primary productivity: experiments under nutrient- and light-limited conditions. Ecology **78**:2326–2338.

Platt, T., D. F. Bird, and S. Sathyendranath. 1991. Critical depth and marine primary production. Proceedings of the Royal Society of London, **B246**:205–217.

Platt, T., C. L. Gallegos, and W. G. Harrison. 1980. Photoinhibition of photosynthesis in natural assemblages of marine phytoplankton. Journal of Marine Research **38**:687–701.

Platt, T., S. Sathyendranath, and P. Ravindran. 1990. Primary production by phytoplankton: analytic solutions for daily rates per unit area of water surface. Proceedings of the Royal Society of London, **B241**:101–111.

Reynolds, C. S. 1984. The ecology of freshwater phytoplankton. Cambridge University Press, Cambridge, UK.

Richter, O., and D. Söndgerath. 1990. Parameter estimation in ecology: the link between data and models. VCH, Weinheim, Germany.

Smetacek, V., and U. Passow. 1990. Spring bloom initiation and Sverdrup's critical-depth model. Limnology and Oceanography **35**:228–234.

Sommer, U. 1993. Phytoplankton competition in Plußsee: a field test of the resource-ratio hypothesis. Limnology and Oceanography **38**:838–845.

Sverdrup, H. U. 1953. On conditions for the vernal blooming of phytoplankton. Journal du Conseil Permanent International pour l'Exploration de la Mer **18**:287–295.

Talling, J. F. 1957. The phytoplankton population as a compound photosynthetic system. New Phytologist **56**:133–149.

———. 1960. Self-shading effects in natural populations of a planktonic diatom. Wetter und Leben **12**:235–242.

———. 1965. The photosynthetic activity of phytoplankton in East African lakes. Internationale Revue der gesamten Hydrobiologie **50**:1–32.

Tilzer, M. M., W. W. Gieskes, R. Heusel, and N. Fenton. 1994. The impact of phytoplankton on spectral water transparency in the Southern Ocean: implications for primary productivity. Polar Biology **14**:127–136.

Webb, W. L., M. Newton, and D. Starr. 1974. Carbon dioxide exchange of *Alnus rubra*: a mathematical model. Oecologia **17**:281–291.

Weissing, F. J., and J. Huisman. 1994. Growth and competition in a light gradient. Journal of Theoretical Biology **168**:323–336.

Wofsy, S. C. 1983. A simple model to predict extinction coefficients and phytoplankton biomass in eutrophic waters. Limnology and Oceanography **28**:1144–1155.